Journal of Applied Statistics
Publication details, including instructions for authors and subscription information:
http://www.tandfonline.com/loi/cjas20

Improved R and s control charts for monitoring the process variance

Guoyi Zhang[a]
[a] Department of Mathematics and Statistics, University of New Mexico, Albuquerque, NM 87131-0001, USA
Published online: 29 Nov 2013.

Journal of Applied Statistics, 2014
Vol. 41, No. 6, 1260–1273, http://dx.doi.org/10.1080/02664763.2013.864264

Improved *R* and *s* control charts for monitoring the process variance

Guoyi Zhang*

Department of Mathematics and Statistics, University of New Mexico, Albuquerque, NM 87131-0001, USA

(*Received 8 January 2013; accepted 6 November 2013*)

The Shewhart *R* control chart and *s* control chart are widely used to monitor shifts in the process spread. One fact is that the distributions of the range and sample standard deviation are highly skewed. Therefore, the *R* chart and *s* chart neither provide an in-control average run length (ARL) of approximately 370 nor guarantee the desired type I error of 0.0027. Another disadvantage of these two charts is their failure in detecting an improvement in the process variability. In order to overcome these shortcomings, we propose the improved *R* chart (IRC) and *s* chart (ISC) with accurate approximation of the control limits by using cumulative distribution functions of the sample range and standard deviation. Simulation studies show that the IRC and ISC perform very well. We also compare the type II error risks and ARLs of the IRC and ISC and found that the *s* chart is generally more efficient than the *R* chart. Examples are given to illustrate the use of the developed charts.

Keywords: *R* chart; *s* chart; average run length; cumulative distribution function; process spread

1. Introduction

The Shewhart *R* control chart (*R* chart) and *s* control chart (*s* chart) [23] are widely used in quality control. The range statistic R_i is defined as the difference between the largest observation and the smallest observation within each subgroup i. Based on the 3σ approach, the control limits of *R* chart is $\mu_R \pm 3\sigma_R$ [25], where μ_R is the mean and σ_R is the standard deviation of R_i. The retrospective upper control limit UCL_R and lower control limit LCL_R of *R* chart can be derived as

$$\mathrm{UCL}_R = D_4\bar{R} \quad \text{and} \quad \mathrm{LCL}_R = D_3\bar{R}, \tag{1}$$

where D_3 and D_4 are constants depending on the subgroup size n, and $\bar{R}$ is an estimate of μ_R.

A viable competitor for the *R* chart is the *s* chart, which uses the average sample standard deviation to estimate process variability σ. The *s* chart tends to detect changes in the process spread quicker but with computational complexity. The retrospective control limits for the *s*

*Email: gzhang123@gmail.com

chart based on $\mu_s \pm 3\sigma_s$ are

$$\text{UCL}_s = B_4\bar{s} \quad \text{and} \quad \text{LCL}_s = B_3\bar{s}, \tag{2}$$

where B_4 and B_3 are constants depending on the subgroup size n, and $\bar{s}$ is an estimate of μ_s.

Both R chart and s chart are based on the assumption that the underlying distribution of the quality characteristic is approximately normal, while, the actual sampling distributions of range R and standard deviation S have long tails on the right side. Even with a normally distributed quality characteristic, the use of the 3σ approach is not appropriate. As shown in [16], the control limits in Equation (1) produce a higher type I error size than that of the $\bar{X}$ chart. The R and s charts could not provide an in-control average run length (ARL) of approximately 370 nor guarantee the type I error size of 0.0027. When sample size is small, the LCLs of R and s charts are truncated to 0 since the skewed distribution of R and S yield negative numbers for the LCLs. Therefore, it is impossible to detect an improvement of the process. Table 1 gives the ARL profiles of R chart through simulation studies (refer to Section 3 for simulation settings). Table 1 shows that the in-control ARLs are all around 200, while the intended value is 370. The chance of the two-sided R chart signaling below the LCL is nearly 0. To overcome these problems and to deal with some special occasions, there has been a rich literature on the control charts. Khoo and Lim [14] proposed an improved R chart (IRC) by using the density function to obtain the control limits based on a desired type I error size. Chan and Cui [10] proposed skewness correction x-bar and R-charts for skewed distributions. Castagliola [8] and Tadikamalla and Popescu [24] discussed improved methods for long-tailed symmetrical distributions of the quality characteristics. Khoo [13] discussed the shortcomings of the conventional s chart and suggested a modified

Table 1. Two-sided and upper-sided R chart's ARL profiles.

	$n = 5$		$n = 10$		$n = 20$	
$\delta = \sigma/\sigma_0$	Upper-sided	Two-sided	Upper-sided	Two-sided	Upper-sided	Two-sided
0.10				1.00		1.00
0.20				1.44		1.00
0.30				6.24		1.03
0.40				33.68		1.66
0.50				163.63		5.12
0.60				650.61		23.40
0.70				2392.34		121.53
0.80				5586.59		648.92
0.90				1282.05		1162.79
1.00	217.34	217.95	223.41	228.15	224.36	209.16
1.05	121.43	123.54	119.21	112.66	98.40	96.76
1.10	73.92	72.50	63.11	63.27	49.35	50.00
1.15	47.84	47.43	37.07	37.95	27.71	27.62
1.20	32.38	32.70	23.97	24.08	16.59	16.71
1.30	17.43	17.35	11.65	11.55	7.55	7.56
1.40	10.60	10.59	6.69	6.67	4.23	4.21
1.50	7.22	7.22	4.37	4.39	2.76	2.76
1.60	5.26	5.26	3.17	3.17	2.02	2.03
1.80	3.33	3.33	2.03	2.02	1.39	1.39
2.00	2.44	2.44	1.55	1.54	1.16	1.16
3.00	1.29	1.29	1.04	1.04	1.00	1.00

s chart for the process variance. Rakitzis and Antzoulakos [17] studied one-sided adaptive *s* control charts for detecting increases or decreases in the process variation. He and Grigoryan [11] and Ahmad *et al.* [6] discussed monitoring variability under double sampling scheme. Acosta-Mejia and Pignatiello [5] proposed modified *R* charts for improved performance, and Lee [15] extended ideas of adaptive control charts to the Shewhart *R* chart for improving the efficiency in signaling increases in the variance. Control charts based on exponentially weighted moving average and cumulative sums (CUSUMs) also gain a lot of attentions, such as [1–4,9,12]. Other techniques are also used in control charts. Riaz and Saghir [19] discussed monitoring process variability using Gini's mean difference. For monitoring changes, Riaz [18] and Riaz and Saghir [20] proposed Shewhart-type control charts based on inter-quartile range and average absolute deviations taken from the median respectively. Schoonhoven *et al.* [22] and Schoonhoven and Does [21] also investigated robust control charts.

Most of the research in the literature are complicated methods which deal with some special occasions. The *R* chart, *s* chart and the improved charts by Khoo and Lim [14] are relatively simple and can be used by people with minimal quantitative backgrounds. These methods are also robust tools, which has been successfully applied in various quality assurance situations. Our proposed research is inspired by the work of Khoo and Lim [14]. One problem from Khoo and Lim's [14] approach is that the density function is obtained by means of the transformed data $Y_i = F(X_i), i = 1, 2, \ldots, n$, in which the cumulative distribution function (CDF) $F(X_i)$ needs to be estimated. To avoid the bias introduced by estimating the parameters, we propose the IRC and improved *s* chart (ISC) by using the CDF of S_i and R_i directly. The precise control limits are derived and the constants needed to construct the control charts are reported.

The present paper is divided into six sections. In Section 2, we propose the IRC and ISC; in Section 3, we use simulation studies to investigate the performance of the proposed control charts. Section 4 gives the comparison between the proposed *R* chart and *s* chart. Section 5 gives two examples. Finally, Section 6 gives a summary of the research.

2. Improved *R* chart and *s* chart

2.1 *Improved R chart*

Assume that there is a series of subgroups. Each of them consists a size n sample, say $X_1, X_2, \ldots, X_n$. Assume that $X_1, X_2, \ldots, X_n$ are independent, identical and normally distributed with mean μ and variance σ_0^2. Without loss of generality, consider n iid standard normal variables $Z_1, \ldots, Z_n$. Let $U = \min Z_i$, $V = \max Z_i$ and $R = V - U$. The joint density function of U and V can be found from [7, p. 218] and is as follows:

$$f(U,V) = \begin{cases} n(n-1)\phi(U)\phi(V)(\Phi(V) - \Phi(U))^{n-2}, & \text{for } V > U, \\ 0, & \text{otherwise,} \end{cases}$$

where ϕ is the probability density function (pdf) of Z_i and Φ is the CDF of Z_i. By transformation, the joint density function of U and R can be shown as follows:

$$g(U,R) = \begin{cases} n(n-1)\phi(U)\phi(U+R)(\Phi(U+R) - \Phi(U))^{n-2}, & \text{for } R > 0, \\ 0, & \text{otherwise.} \end{cases}$$

The marginal CDF of R can be derived as follows:

$$\begin{aligned} H_R(r) &= P(R < r) \\ &= \int_0^r \int_{-\infty}^{\infty} g(U,R)\, \mathrm{d}U\, \mathrm{d}R \end{aligned}$$

$$= \int_{-\infty}^{\infty} \int_{0}^{r} n(n-1)\phi(U)\phi(U+R)(\Phi(U+R)-\Phi(U))^{n-2}\,\mathrm{d}R\,\mathrm{d}U$$
$$= \int_{-\infty}^{\infty} n\phi(U)(\Phi(U+R)-\Phi(U))^{n-1}\,\mathrm{d}U. \quad (3)$$

For a one-sided IRC, the upper control limit $\mathrm{UCL}_{\mathrm{RIU}}$ can be derived by solving the following equation:

$$\int_{-\infty}^{\infty} n\phi(U)(\Phi(U+r)-\Phi(U))^{n-1}\,\mathrm{d}U = 1-\alpha, \quad (4)$$

for r, say D_{U}^{*} , where α is the type I error. The lower control limit $\mathrm{LCL}_{\mathrm{RIL}}$ can be derived by solving

$$\int_{-\infty}^{\infty} n\phi(U)(\Phi(U+r)-\Phi(U))^{n-1}\,\mathrm{d}U = \alpha, \quad (5)$$

for r, say D_{L}^{*}. The upper-sided and lower-sided IRC's limits are computed as

$$\mathrm{UCL}_{\mathrm{RIU}} = {D_{\mathrm{U}}}^{*}\sigma \quad \text{and} \quad \mathrm{LCL}_{\mathrm{RIL}} = {D_{\mathrm{L}}}^{*}\sigma. \quad (6)$$

For a two-sided IRC, the control limits $\mathrm{UCL}_{\mathrm{RIT}}$ and $\mathrm{LCL}_{\mathrm{RIT}}$ can be obtained by Equations (4) and (5), respectively, with the type I error in both equations replaced by $\alpha/2$. The two-sided IRC's limits are

$$\mathrm{UCL}_{\mathrm{RIT}} = D_{2}^{*}\sigma \quad \text{and} \quad \mathrm{LCL}_{\mathrm{RIT}} = D_{1}^{*}\sigma, \quad (7)$$

and the two-sided retrospective IRC's limits are

$$\mathrm{UCL}_{\mathrm{RIT}} = D_{4}^{*}\bar{R} \quad \text{and} \quad \mathrm{LCL}_{\mathrm{RIT}} = D_{3}^{*}\bar{R}. \quad (8)$$

We use the *R* program to evaluate the integrals in Equations (4) and (5) and report the constants $D_1^* - D_4^*$, D_{U}^* and D_{L}^* corresponding to the type I error sizes of 0.0027 and 0.005 in Tables 2 and 3, respectively.

2.2 *Improved s chart*

Consider next estimating σ based on the sample variance of a process $S^2 = \sum_{i=1}^{n}(X_i - \bar{X})^2/(n-1)$. The standard probability theory [7] says that $(n-1)S^2/\sigma^2 \sim \chi^2_{n-1}$. Let W be a χ^2 distribution with $n-1$ degrees of freedom, i.e. $W \sim \chi^2_{n-1}$. S has the same distribution as $\sigma\sqrt{W}/\sqrt{n-1}$. The CDF of S for the standard normal variables $Z_1, Z_2, \ldots, Z_n$ is

$$\begin{aligned} H_S(s) &= P(S < s) \\ &= P\left(\frac{1}{\sqrt{n-1}}\sqrt{W} < s\right) \\ &= P\{W < (n-1)s^2\} \\ &= G_{\chi^2_{n-1}}\{(n-1)s^2\}, \end{aligned}$$

where $G(\cdot)$ is the CDF of the χ^2 distribution with $n-1$ degrees of freedom.

Table 2. Values of LCL and UCL constants, and $D_1^* - D_4^*$ for the IRC.

n	D_1^*	D_2^*	D_L^*	D_U^*	D_3^*	D_4^*
2	0.0024	4.5477	0.0047	4.2502	0.0021	4.0316
3	0.0701	4.9642	0.0990	4.6858	0.0414	2.9322
4	0.2207	5.2132	0.2784	4.9453	0.1072	2.5319
5	0.3967	5.3906	0.4735	5.1298	0.1706	2.3175
6	0.5692	5.5280	0.6576	5.2725	0.2246	2.1815
7	0.7290	5.6398	0.8246	5.3885	0.2696	2.0857
8	0.8746	5.7340	0.9746	5.4861	0.3072	2.0141
9	1.0066	5.8152	1.1094	5.5702	0.3389	1.9580
10	1.1265	5.8863	1.2311	5.6439	0.3660	1.9124
11	1.2359	5.9499	1.3414	5.7095	0.3895	1.8752
12	1.3361	6.0070	1.4422	5.7686	0.4101	1.8438
13	1.4283	6.0589	1.5346	5.8223	0.4281	1.8162
14	1.5135	6.1065	1.6199	5.8714	0.4442	1.7923
15	1.5926	6.1504	1.6988	5.9167	0.4587	1.7714
20	1.9182	6.3293	2.0228	6.1013	0.5136	1.6946
25	2.1645	6.4641	2.2669	6.2401	0.5506	1.6444

Notes: D_L^* denotes the one-sided LCL constant and D_U^* denotes the one-sided UCL constant. The type I error risk is 0.0027 ($ARL_0 = 370$).

Table 3. Values of LCL, UCL and $D_1^* - D_4^*$ for the IRC.

n	D_1^*	D_2^*	D_L^*	D_U^*	D_3^*	D_4^*
2	0.0045	4.2843	0.0088	3.9743	0.0040	3.7981
3	0.0953	4.7177	0.1348	4.4285	0.0563	2.7866
4	0.2713	4.9759	0.3427	4.6982	0.1318	2.4167
5	0.4642	5.1596	0.5549	4.8896	0.1996	2.2182
6	0.6470	5.3017	0.7489	5.0374	0.2553	2.0922
7	0.8133	5.4172	0.9218	5.1575	0.3008	2.0034
8	0.9628	5.5144	1.0752	5.2583	0.3382	1.9369
9	1.0973	5.5981	1.2121	5.3452	0.3695	1.8849
10	1.2188	5.6716	1.3349	5.4213	0.3960	1.8426
11	1.3291	5.7369	1.4459	5.4890	0.4189	1.8080
12	1.4298	5.7958	1.5469	5.5500	0.4389	1.7789
13	1.5222	5.8492	1.6393	5.6053	0.4563	1.7534
14	1.6074	5.8982	1.7244	5.6559	0.4718	1.7312
15	1.6864	5.9433	1.8031	5.7026	0.4857	1.7118
20	2.0107	6.1272	2.1250	5.8926	0.5383	1.6405
25	2.2550	6.2656	2.3667	6.0353	0.5736	1.5939

Notes: D_L^* denotes the one-sided LCL constant and D_U^* denotes the one-sided UCL constant. The type I error risk is 0.005 ($ARL_0 = 200$).

For a one-sided ISC, the upper control limit UCL_{sIU} can be derived by solving the following equation:

$$G_{\chi^2_{n-1}}\{(n-1)s^2\} = 1 - \alpha, \tag{9}$$

Table 4. Values of LCL, UCL and $B_3^* - B_6^*$ for the ISC.

n	B_5^*	B_6^*	B_L^*	B_U^*	B_3^*	B_4^*
2	0.0017	3.2049	0.0033	2.9997	0.0021	4.0167
3	0.0368	2.5704	0.0520	2.4318	0.0415	2.9005
4	0.0996	2.2825	0.1256	2.1722	0.1081	2.4775
5	0.1627	2.1094	0.1941	2.0155	0.1731	2.2440
6	0.2183	1.9910	0.2520	1.9081	0.2294	2.0925
7	0.2657	1.9034	0.3003	1.8285	0.2769	1.9839
8	0.3063	1.8353	0.3410	1.7666	0.3174	1.9019
9	0.3412	1.7804	0.3756	1.7166	0.3520	1.8368
10	0.3715	1.7350	0.4054	1.6752	0.3819	1.7837
11	0.3981	1.6966	0.4314	1.6401	0.4081	1.7394
12	0.4216	1.6635	0.4543	1.6100	0.4313	1.7016
13	0.4426	1.6347	0.4746	1.5837	0.4519	1.6691
14	0.4615	1.6094	0.4929	1.5605	0.4704	1.6406
15	0.4786	1.5868	0.5094	1.5398	0.4872	1.6154
20	0.5450	1.5021	0.5730	1.4624	0.5522	1.5220
25	0.5911	1.4457	0.6168	1.4107	0.5973	1.4609

Notes: B_L^* denotes the one-sided LCL constant and B_U^* denotes the one-sided UCL constant. The type I error risk is 0.0027 ($ARL_0 = 370$).

for s, say B_U^* . The lower control limit LCL_{sIL} can be derived by solving

$$G_{\chi^2_{n-1}}\{(n-1)s^2\} = \alpha, \tag{10}$$

for s, say B_L^*. For a two-sided ISC, the control limits UCL_{sIT} and LCL_{sIT} can be obtained by solving Equations (9) and (10), respectively, with the type I error α replaced by $\alpha/2$. The upper-sided and lower-sided ISC 's limits are computed as

$$UCL_{sIU} = {B_U}^*\sigma \quad \text{and} \quad UCL_{sIL} = {B_L}^*\sigma. \tag{11}$$

The two-sided ISC 's limits are computed as

$$UCL_{sIT} = B_6^*\sigma \quad \text{and} \quad LCL_{sIT} = B_5^*\sigma. \tag{12}$$

The retrospective two-sided ISC's limits are

$$UCL_{sIT} = B_4^*\bar{s} \quad \text{and} \quad LCL_{sIT} = B_3^*\bar{s}, \tag{13}$$

where constants $B_3^* - B_6^*$, B_U^* and B_L^* corresponding to the type I errors of 0.0027 and 0.005 are provided in Tables 4 and 5, respectively.

3. Simulation studies: performance of the improved charts

In this section we use simulations to evaluate the proposed R chart and s chart. Simulation settings follow from [14]. Let σ_0 be the nominal standard deviation (in our case, $\sigma_0 = 1$) and σ be the shifted process standard deviation. The magnitude of shifts in the process variability δ is defined as σ/σ_0. When $\delta = 1.0$, the process is in-control. Without loss of generality, we assume that the observations for the in control cases follow a standard normal distribution. Simulations are

Table 5. Values of LCL and UCL constants, and $B_3^* - B_6^*$ for the ISC.

n	B_5^*	B_6^*	B_{L}^*	B_{U}^*	B_3^*	B_4^*
2	0.0032	3.0234	0.0062	2.8071	0.0040	3.7892
3	0.0501	2.4478	0.0707	2.3019	0.0565	2.7621
4	0.1224	2.1849	0.1546	2.0687	0.1329	2.3715
5	0.1904	2.0264	0.2274	1.9275	0.2026	2.1557
6	0.2480	1.9176	0.2869	1.8303	0.2606	2.0153
7	0.2963	1.8371	0.3355	1.7582	0.3088	1.9148
8	0.3369	1.7745	0.3759	1.7021	0.3491	1.8389
9	0.3716	1.7239	0.4099	1.6567	0.3834	1.7785
10	0.4015	1.6821	0.4390	1.6190	0.4128	1.7293
11	0.4275	1.6466	0.4643	1.5871	0.4383	1.6881
12	0.4505	1.6161	0.4864	1.5597	0.4608	1.6531
13	0.4710	1.5896	0.5061	1.5357	0.4809	1.6230
14	0.4893	1.5661	0.5236	1.5146	0.4988	1.5964
15	0.5059	1.5452	0.5394	1.4957	0.5150	1.5730
20	0.5698	1.4670	0.6001	1.4251	0.5774	1.4865
25	0.6139	1.4148	0.6418	1.3778	0.6204	1.4297

Notes: B_{L}^* denotes the one-sided LCL constant and B_{U}^* denotes the one-sided UCL constant. The type I error risk is 0.005 ($\mathrm{ARL}_0 = 200$).

performed based on 1,000,000 replications with the following factors: (1) in-control $\mathrm{ARL}_0 = 370$; (2) sample sizes: $n = 5, 10$ and 20 and (3) δ: $\delta \in \{1.05, 1.10, 1.15, \ldots, 3\}$ (increasing shifts) or $\delta \in \{0.9, 0.8, 0.7, \ldots, 0.1\}$ (decreasing shifts).

In the following, we use two-sided IRC to illustrate how we calculate the ARL. First, we generate the data under different settings based on the magnitude of shifts in the process variability and sample size. Then we calculate the range statistic R_i and use Equation (7) to compute the control limits to see if R_i is within the limits or not. Repeat the process 1,000,000 times. The reciprocal of the proportion of times that R_i is beyond the limits is the ARL. The upper, lower and two-sided IRC control limits are derived by Equations (6) and (7). The upper, lower and two-sided ISC control limits are derived by Equations (11) and (12).

Tables 6 and 7 give the ARL profiles of IRC and ISC, respectively. From Tables 6 and 7, we can see that the in-control ARLs are all around 370. The ARL values become smaller as the magnitude of shift increases or decreases. We also observe that with increased sample size, the sensitivity of the chart also increases.

4. Comparison between the IRC and ISC

In this section, we compare IRC and ISC by examining the type II error risks and the ARLs. Let R_α and s_α be the solutions of Equations (4) and (9), respectively. The type II error risk of the R chart is

$$P(R < R_\alpha | \delta = \sigma) = \int_{-\infty}^{\infty} nf(U)(F(R_\alpha + U) - F(U))^{n-1}\,\mathrm{d}U, \tag{14}$$

where $f(\cdot)$ and $F(\cdot)$ are the pdf and CDF functions of the $N(0, \sigma^2)$ distribution, respectively.

Table 6. ARL profiles of the IRC, in-control ARL (ARL_0) = 370.

	$n = 5$			$n = 10$			$n = 20$		
$\delta = \sigma/\sigma_0$	Upper-sided	Lower-sided	Two-sided	Upper-sided	Lower-sided	Two-sided	Upper-sided	Lower-sided	Two-sided
0.10		1.00	1.04		1.00	1.00		1.00	1.00
0.2		1.81	2.66		1.00	1.00		1.00	1.00
0.3		4.94	8.58		1.11	1.23		1.00	1.00
0.4		12.32	23.08		1.89	2.53		1.04	1.08
0.5		27.11	51.96		4.39	6.75		1.45	1.71
0.6		52.47	101.99		11.21	19.12		3.06	4.20
0.7		93.54	181.22		28.91	52.19		8.67	13.60
0.8		156.05	301.02		71.02	134.53		28.72	50.44
0.9		243.19	423.90		166.77	308.45		101.40	188.04
1.0	371.33	377.35	369.41	376.36	372.99	372.70	374.81	367.91	371.74
1.05	198.80		266.38	181.91		258.73	154.79		248.50
1.10	116.48		172.68	92.94		148.12	77.08		127.59
1.15	72.55		110.96	53.59		87.26	40.57		66.21
1.20	47.28		73.80	33.07		52.27	23.69		37.91
1.30	23.94		35.50	15.15		22.35	9.93		14.32
1.40	13.86		19.61	8.33		11.53	5.26		7.11
1.50	9.06		12.23	5.24		6.89	3.28		4.17
1.60	6.40		8.30	3.67		4.63	2.32		2.78
1.80	3.87		4.70	2.24		2.62	1.50		1.68
2.00	2.73		3.17	1.66		1.84	1.21		1.28
3.00	1.34		1.41	1.05		1.07	1.00		1.00

The type II error risk of the sample standard deviation S is

$$P(S < s_\alpha | \delta = \sigma) = P\left(W < \frac{Q_{n-1}(1-\alpha)}{\sigma^2}\right), \tag{15}$$

where $Q(\cdot)$ is the quantile function of the χ^2 distribution with $n-1$ degrees of freedom. Let $D_n(\sigma) = P(R < R_\alpha | \delta = \sigma) - P(S < s_\alpha | \delta = \sigma)$ be the difference between the type II error risks of the IRC and ISC. Figure 1 plots $D_n(\sigma)$ versus the process spread σ ranging from 1 to 5 with different sample sizes $n = 5, 10$ and 20 for the upper-sided case. The dot dash curve, dash curve and regular curve are associated with sample sizes $n = 20, n = 10$ and $n = 5$, respectively. We see from Figure 1 that with an increase in the process spread, $D_n(\sigma)$ increases to a maximum then decreases until there is almost no difference between the type II error risks. The larger the sample size, the larger the maximum value of $D_n(\sigma)$, and the earlier the maximum value of $D_n(\sigma)$ is reached. The s chart is more effective (with greater power) when the sample size is large. When the process spread is large enough, there is almost no difference between the two charts. Figure 2 plots $D_n(\sigma)$ versus the process spread σ ranging from 0.1 to 1 for the lower-sided case. Figure 2 reveals that the s chart is more effective (with greater power) when the sample size is large; there is almost no difference between the two charts when the process spread is small enough; the larger the sample size, the larger the maximum value of $D_n(\sigma)$, and the slower the maximum value of $D_n(\sigma)$ is reached. Figure 3 plots $D_n(\sigma)$ versus σ ranging from 0.1 to 5 for different sample sizes for the two-sided case. The shape in Figure 3 is basically a combination of Figures 1 and 2 with an additional finding that the maximum of the difference between the type

Table 7. ARL profiles of the ISC, in-control ARL (ARL_0) = 370.

	$n = 5$			$n = 10$			$n = 20$		
$\delta = \sigma/\sigma_0$	Upper-sided	Lower-sided	Two-sided	Upper-sided	Lower-sided	Two-sided	Upper-sided	Lower-sided	Two-sided
0.1		1.00	1.03		1.00	1.00		1.00	1.00
0.2		1.78	2.62		1.00	1.00		1.00	1.00
0.3		4.90	8.45		1.06	1.14		1.00	1.00
0.4		12.27	22.62		1.70	2.27		1.00	1.01
0.5		26.98	51.79		3.97	6.14		1.19	1.34
0.6		53.00	103.07		10.41	17.71		2.31	3.10
0.7		93.01	185.49		27.52	49.66		6.76	10.58
0.8		155.15	307.97		69.54	129.11		24.24	42.94
0.9		245.21	444.64		166.77	300.21		95.36	174.67
1.0	372.21	366.16	368.18	368.59	370.91	367.78	374.95	372.85	368.36
1.05	184.80		263.01	156.32		225.27	120.59		187.23
1.10	107.08		157.38	75.37		120.29	48.40		78.82
1.15	65.45		99.95	41.86		63.97	23.07		35.54
1.20	42.95		64.13	24.35		36.73	12.57		18.32
1.30	21.22		30.48	10.82		14.99	5.15		6.72
1.40	12.28		16.85	5.96		7.76	2.83		3.43
1.50	8.01		10.49	3.82		4.74	1.92		2.20
1.60	5.73		7.20	2.75		3.26	1.50		1.64
1.80	3.49		4.16	1.80		2.01	1.16		1.20
2.00	2.50		2.87	1.41		1.51	1.05		1.07
3.00	1.29		1.35	1.02		1.03	1.00		1.00

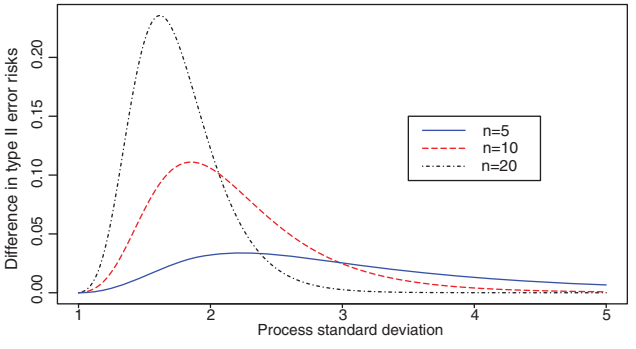

Figure 1. Plot of difference in type II error risks between the IRC and ISC versus the process standard deviation, upper-sided.

II error risks is larger when $\sigma \in (1, 5)$ than that with $\sigma \in (0, 1)$. When the sample size is large, the range (which only use the maximum observation and minimum observation) is not enough to deliver the sample information compared with the sample standard deviation. Therefore, the *s* chart is more effective than the *R* chart under a large sample size.

Figure 4 plots the difference in ARLs defined as ARL(IRC)–ARL(ISC), versus the process standard deviation σ ranging from 0.1 to 5 under different sample sizes for the two-sided case. Figure 4 in general reveals similar findings as Figures 1–3 except that the *R* chart looks more

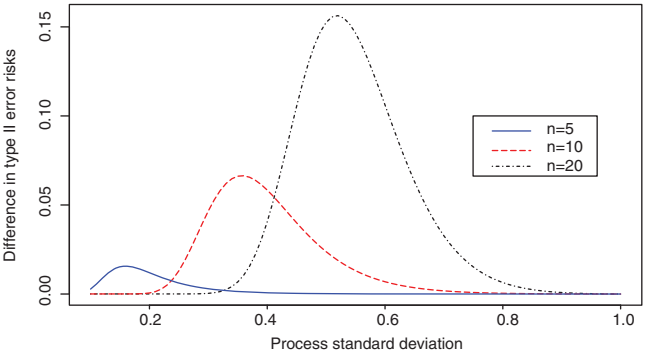

Figure 2. Plot of difference in type II error risks between the IRC and ISC versus the process standard deviation, lower-sided.

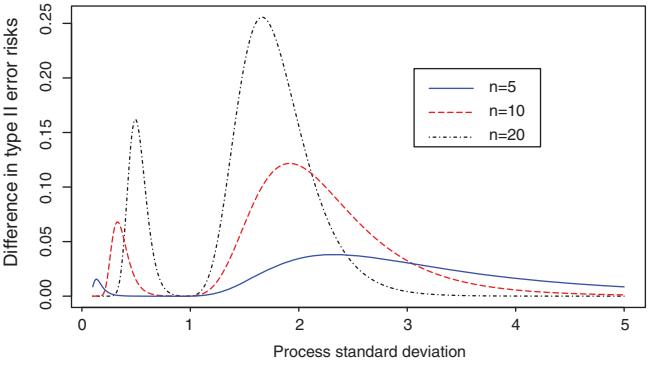

Figure 3. Plot of difference in type II error risks between the IRC and ISC versus the process standard deviation, two-sided.

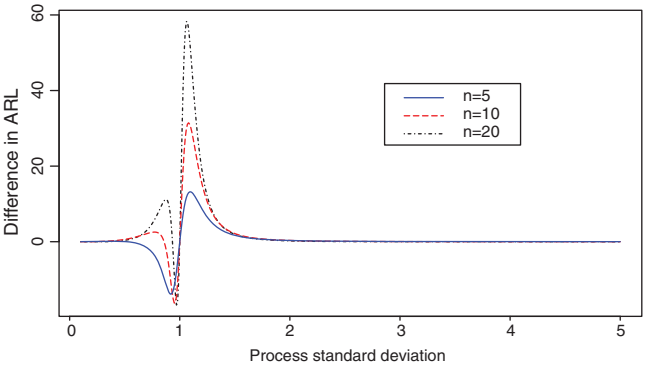

Figure 4. Plot of difference in ARL between the IRC and ISC versus the process standard deviation.

effective in detecting signals when process standard deviation is between 0.6 and 1. This is because a small change in the probability not shown in the type II error size figures may lead to a big change in the ARL values. For example, when the standard deviation shifted slightly from $\sigma = 1$, the difference in type II error size is negligible, therefore not shown in Figures 1–3; while, the difference in reciprocal of the powers are large enough to be detected by Figure 4. Figure 4 indicates that ISC is not uniformly more efficient than IRC.

Table 8. An illustrative example: simulated data.

Subgroup No., j	Observations					Range
	X_1	X_2	X_3	X_4	X_5	R_j
1	1.404	−1.426	0.624	1.489	0.454	2.915
2	0.653	−1.768	0.814	−0.224	0.531	2.421
3	−0.082	1.332	1.146	−0.721	1.816	2.537
4	−0.912	−1.245	−0.932	−0.976	0.735	1.980
5	−0.621	−0.935	−0.080	−1.076	0.742	1.818
6	−2.464	−1.087	−1.278	−4.671	−3.110	3.584
7	−1.697	−1.656	−0.862	3.117	2.738	4.814
8	2.558	0.566	−0.099	1.701	−1.772	4.33
9	−0.963	0.359	0.812	0.797	−0.203	1.775
10	−4.107	3.126	−3.466	1.682	−0.782	7.233
11	1.047	0.185	0.617	0.557	3.022	2.837
12	3.279	−2.259	0.847	−4.152	1.583	7.431
13	−2.821	1.719	0.201	0.739	0.567	4.54
14	0.368	1.493	−0.040	−1.639	4.485	6.124
15	4.947	1.723	1.183	4.658	1.738	3.764
16	1.259	0.922	2.740	−0.233	−0.067	2.973
17	−2.168	−1.410	0.130	2.240	2.451	4.619
18	−1.870	1.009	−4.670	−0.002	0.096	5.679
19	−3.479	1.546	−1.482	1.842	−2.756	5.321
20	1.861	0.946	1.135	0.035	0.780	1.826

5. Example of application

5.1 *Simulated data application*

In this section, we describe an example (follows from [14]) to illustrate the usage of the IRC in practice. The application of the s chart is similar. We simulated 20 subgroups of size 5, with the first 5 subgroups in-control (iid observations from $N(0,1)$) and the next 15 subgroups out-of-control. For out-of-control process, the shift magnitude $\delta = \sigma/\sigma_0 = 2$. We report the simulated data X_1, X_2, X_3, X_4, X_5 and the corresponding ranges, $R_j, j = 1, 2, \ldots, 20$, in Table 8. Now we

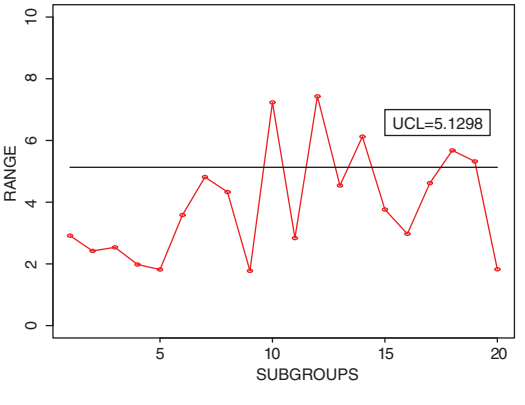

Figure 5. An IRC for the range R_j (statistics are in Table 8).

Table 9. Summary statistics for 20 samples of five surface roughness measurements on reamed holes (in.).

Sample	$\bar{x}$	$\tilde{x}$	R	s
1	34.6	35	9	3.4
2	46.8	45	23	8.8
3	32.6	34	12	4.6
4	42.6	41	6	2.7
5	26.6	28	5	2.4
6	29.6	30	2	0.9
7	33.6	31	13	6.0
8	28.2	30	5	2.5
9	25.8	26	9	3.2
10	32.6	30	15	7.5
11	34.0	30	22	9.1
12	34.8	35	5	1.9
13	36.2	36	3	1.3
14	27.4	23	24	9.6
15	27.2	28	3	1.3
16	32.8	32	5	2.2
17	31.0	30	6	2.5
18	33.8	32	6	2.7
19	30.8	30	4	1.6
20	21.0	21	2	1.0

want to derive a one-sided IRC for monitoring increases in the process variance with $\mathrm{ARL}_0 = 370$. By Equation (4), $\mathrm{UCL}_{\mathrm{RIU}}$ is found to be 5.1298.

Figure 5 presents a plot of the range statistics R_j versus the subgroups. We see from Figure 5 that the first out-of-control signal alarmed at subgroup 10.

5.2 *Real data application*

This example is about monitoring the surface roughness of reamed holes [25, p. 67]. Dohm *et al.* worked with a manufacturer on a project involving roughness measurement after the reaming of

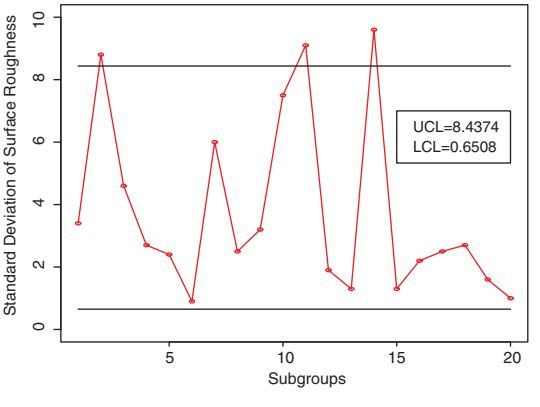

Figure 6. An ISC for the standard deviation s_j (statistics are available from Table 9).

preformed holes in a particular metal part. Table 9 contains some summary statistics (the sample mean $\bar{x}$, sample median $\tilde{x}$, sample range R and the sample standard deviation s) for 20 samples (taken over a period of 10 days) of $n = 5$ consecutive reamed holes.

We are interested in developing a two-sided ISC for monitoring shifts in the process variance with $\mathrm{ARL}_0 = 370$. The 20 samples in Table 9 have $\bar{s} = 3.76$. Using Table 4, for $n = 5$ one has $B_4^* = 2.244$ and $B_3^* = 0.1731$. Therefore, the upper control limit $\mathrm{UCL}_{\mathrm{sIU}} = B_4^*\bar{s} = 8.4374$ and the lower control limit $\mathrm{LCL}_{\mathrm{sIL}} = B_3^*\bar{s} = 0.6508$. Figure 6 is a retrospective s chart for the sample standard deviations in Table 9. From Figure 6, we can see that the chart signals an out-of-control at subgroup 2 for the first time.

6. Conclusions

The R chart and s chart suffer from two main disadvantages: (1) the actual in-control ARL is much lower than expected; (2) impossible in detecting an improvement in the process. In this research, we propose the IRC and ISC by using the CDF of the range and sample standard deviation to construct the control limits. The constants used to construct the control limits are provided. Simulation results show that the proposed methods work very well. ISC has been shown to be more effective than IRC in general, and is recommended for use with large sample sizes.

Acknowledgements

The author thanks the referees for their very careful reading of the manuscript and would like to express his sincere appreciation for their insightful and helpful comments.

References

[1] N. Abbas, M. Riaz, and R.J.M.M. Does, *CS-EWMA chart for monitoring process dispersion*, Qual. Reliab. Eng. Int. 29 (2013), pp. 653–663.
[2] N. Abbas, M. Riaz, and R.J.M.M. Does, *Memory-type control charts for monitoring the process dispersion*, Qual. Reliab. Eng. Int. 29(5) (2013), pp. 653–663.
[3] S.A. Abbasi and A. Miller, *MDEWMA chart: An efficient and robust alternative to monitor process dispersion*, J. Stat. Comput. Simul. 83 (2013), pp. 247–268.
[4] S.A. Abbasi, M. Riaz, and A. Miller, *Enhancing the performance of CUSUM scale chart*, Comput. Ind. Eng. 63 (2012), pp. 400–409.
[5] C.A. Acosta-Mejia and J.J. Pignatiello, *Modified R charts for improved performance*, Qual. Eng. 20 (2008), pp. 361–369.
[6] S. Ahmad, M. Riaz, S.A. Abbasi, and Z.Y. Lin, *On monitoring process variability under double sampling scheme*, Int. J. Prod. Econ. 142 (2013), pp. 388–400.
[7] L.J. Bain and M. Engelhardt, *Introduction to Probability and Mathematical Statistics*, 2nd ed., Duxbury, Pacific Grove, CA, 1992.
[8] P. Castagliola, *Control Charts for Data Having a Symmetrical Distribution with a Positive Kurtosis, Recent Advances in Reliability and Quality Engineering*, World Scientific Publishers, Hackensack, NJ, 2001, pp. 1–16.
[9] P. Castagliola, G. Celano, and S. Fichera, *A new CUSUM-S2 control chart for monitoring the process variance*, J. Qual. Maint. Eng. 15 (2009), pp. 344–357.
[10] L.K. Chan and H.J. Cui, *Skewness correction x-bar and R-charts for skewed distributions*, Naval Res. Log. 50 (2003), pp. 555–573.
[11] D. He and A. Grigoryan, *An improved double sampling s chart*, Int. J. Prod. Res. 41 (2003), pp. 2663–2679.
[12] L. Huwang, C.J. Huang, and Y.H.T. Wang, *New EWMA control charts for monitoring process dispersion*, Comput. Stat. Data Anal. 54 (2010), pp. 2328–2342.
[13] M.B.C. Khoo, *A modified s chart for the process variance*, Qual. Eng. 17 (2005), pp. 567–577.
[14] M.B.C. Khoo and E.G. Lim, *An improved R (range) control chart for monitoring the process variance*, Qual. Reliab. Eng. Int. 21 (2005), pp. 43–50.
[15] P. Lee, *Adaptive R charts with variable parameters*, Comput. Stat. Data Anal. 55 (2011), pp. 2003–2010.

[16] D.C. Montgomery, *Introduction to Statistical Quality Control*, 6th ed., Wiley, New York, 2008.
[17] A.C. Rakitzis and D.L. Antzoulakos, *On the improvement of one-sided S control charts*, J. Appl. Stat. 38 (2011), pp. 2839–2858.
[18] M. Riaz, *A dispersion control chart*, Commun. Stat. Simul. Comput. 37 (2008), pp. 1239–1261.
[19] M. Riaz and A. Saghir, *Monitoring process variability using Gini's mean difference*, Qual. Technol. Quant. Manage. 4 (2007), pp. 439–454.
[20] M. Riaz and A. Saghir, *A mean deviation based approach to monitor process variability*, J. Stat. Comput. Simul. 79 (2009), pp. 1173–1193.
[21] M. Schoonhoven and R.J.M.M. Does, *A robust standard deviation control chart*, Technometrics 54 (2012), pp. 73–82.
[22] M. Schoonhoven, M. Riaz, and R.J.M.M. Does, *Design and analysis of control charts for standard deviation with estimated parameters*, J. Qual. Technol. 43 (2011), pp. 307–333.
[23] W.A. Shewhart, *Economic Control of Quality of Manufacturing Processes*, John Wiley & Sons, Milwaukee, 1931.
[24] P. Tadikamalla and D. Popescu, *Kurtosis correction method for x-bar and R control charts for long-tailed symmetrical distributions*, Naval Res. Log. 54 (2007), pp. 371–383.
[25] S.B. Vardeman and J.M. Jobe, *Statistical Quality Assurance Methods for Engineers*, John Wiley & Sons, Inc., New York, 1999.